Oscillations of a Spacecraft with a Vertical Elastic Tether

Vladimir S. Aslanov

Department of Theoretical Mechanics, Samara State Aerospace University, 34, Moscovskoe shosse, Samara, 443086, Russia (e-mail: aslanov_vs@mail.ru)

Abstract. The motion about a centre of mass of a spacecraft with a vertical elastic tethered system under the action of the gravitational moment and small periodic tethered force at a circular orbit is studied. The mathematical model is derived using Lagrange's equations including tether vibrations and oscillations of the spacecraft relatively of the proper mass center. The paper contains bifurcation analysis, phase space study, and analytic solutions for separatrixes. The considered mechanical system performs chaotic motion near separatrixes under the influence of small disturbances. The Melnikov method gives a criterion for homo/heteroclinic chaos in terms of system parameters. Results of the study can be useful for the analysis of gravitational stabilization systems with space tethers and for studying the behavior of a spacecraft with a deployed tether.

Keywords: Chaos, Oscillation, Spacecraft, Tethered system.
PACS: 02.30.Gp, Special functions; 02.60.Lj, Ordinaryand partial differential equations; boundary value problems; 02.40.Ma, Global differential geometry; 02.30.Rz, Integral equations; 02.30.Lt, Sequences, series, and summability; 02.30.Mv, Approximations and expansions

INTRODUCTION

The field of space tethers has received very much attention in recent decades, with many specialist articles and books available in the scientific literature. The fundamental paper by V. Beletsky and E. Levin [1] has played an important role in providing the basis for the study of the tethered system dynamics. Modern results and new problem statements of the study of tethers dynamics are also very important. A new concept for the application of space tethers in planetary exploration and payload transfer is presented in Williams, Blanksby and Trivailo [2]. It is proposed that a payload be deployed on a spinning tether in a hyperbolic orbit in order to provide a sufficient increment of a velocity such that it is captured in an elliptical orbit at the destination planet. Due to conservation of momentum, the main spacecraft gains a so-called "momentum-enhanced gravity-assist". This concept is investigated by conducting numerical simulations of a simplified system. The mathematical model is derived using Lagrange's equations including tether mass, but neglects tether vibrations. Tether-mediated rendezvous between a noncooperative payload and a maneuverable tether is considered by Williams [3]. Practical scenarios in which the tether system orbit and payload are inclined relative to each other mean that capture is no longer limited to the orbital plane. The necessary conditions for achieving a zero

position and zero velocity rendezvous when the tether system and payload are in arbitrary orbits are derived. It is shown that significant manipulation of the three-dimensional dynamics can be achieved in under two orbits using only tension control with smooth variations in tether length. At the most basic level, it has been shown to be conceptually feasible to boost or deorbit a payload by means of a long tether. A simple example is the deployment of a payload from a large spacecraft, utilizing the tether swing motion (librations) to generate the delta-v required to have the payload re-enter the Earth's atmosphere (Williams, Blanksby, and Trivailo [2], Zimmerman, Schottle, and Messerschmid [4]). The central advantage of using tethers in many of these applications is that very little fuel needs to be consumed. The benefits of using tethers are reaped over multiple missions by reusing the same tether. A method of damping structural vibrations using optimization techniques is presented and applied to a tethered satellite system given by Dignath and Schiehlen [5]. Misra [6] successfully studied dynamics and control of two-body and *n*-body tethered satellites. In addition nonlinear roll and pitch motions of two-body systems are examined. The YES2 (2nd Young Engineers' Satellite) tether system is the first European tether hardware operated in space in the 2007. The YES2 tether is non-conductive, 31.7 km long with a diameter of 0.5mm and weighs only 5.8 kg. To initiate the deployment a spring-based ejection system was developed, and to apply accurate momentum transfer a timer and release system is present on the subsatellite side. A small, 6 kg re-entry capsule was developed as subsatellite. Confidence is gained from the mission results for use of the deployer in future missions. There are many potential applications for tethers such as coordinated measurements from multiple satellites tethered together (formation flying), artificial gravity in spacecraft using a rotating tethered system, small pay-load launch assist e.g. [7,8]. The tethered systems offer numerous ways of beneficial implementation on modern spacecrafts and allow to perform multiple tasks such as the tethered payload planetary capture applications, studied by Williams [9]. Thus Space tethers have been proposed for a wide range of useful applications, including payload delivery from the Earth orbit and Earth monitoring, using surveillance equipment on the lower end of a vertical tether. Majority of recently developed models are focused on the tether, while the spacecraft and the payload are usually referred to as the point end-masses [1-9].

However, the study of the motion of a spacecraft with a tether relative of the own mass center is very important in modern science. The motion about of a mass centre of a spacecraft with a tethered system, designed to launch a re-entry capsule from a circular orbit was considered in [10, 11]. The direction and value of the tethered force is varied in the deployment of the tethered system. If the point of application of the tethered force does not coincide with of the mass centre of the spacecraft, then oscillations with variable amplitude and frequency occur. The approximate solutions of the equations of motion about of the mass center the spacecraft obtained by Aslanov [10, 11]. These solutions can be used for the determination an undesirable additional microaccelerations. In these articles the nonelastic tether is considered and the spacecraft moves at a circular orbit.

In this paper we consider a tethered system consisting of a spacecraft and a payload connected with a variable-length elastic tether. In general, tether dynamics are very complex. A flexible tether undergoes a complicated set of coupled vibrations. These

may be separated into longitudinal, lateral, and rigid body modes [12]. All three of these vibratory modes are coupled due to the influence of the gravity gradient. Herein we will study the oscillations of a spacecraft as a rigid body under the action of the tethered force and gravitational moment. If the tether is extensible, then vibrations of the tether initiate small periodic disturbances, affecting the spacecraft. On the other hand, depending on the ratio between the spacecraft's moments of inertia and tethered system parameters, points of unstable equilibrium can appear in phase space. These two factors lead to chaos [13, 14] and irregular behavior of the spacecraft in its motion about a centre of mass. The purpose of this paper is to research the influence of elastic fluctuations of the tether on chaotic behavior of the spacecraft.

MATEMATICAL MODEL

The equations governing the dynamics of the tethered system are highly nonlinear. Hence the dynamical behavior is very rich and in some cases can be chaotic. The general dynamics of such systems involves pitch and roll motions of the tether, longitudinal and transverse elastic oscillations of the tether and three-dimensional attitude dynamics of the end-bodies. Pitch and roll motions of the tether are only marginally affected by the elastic oscillations of the tether and the rigid body dynamics of the end-bodies. We study the motion of the spacecraft relative the mass center under the influence of longitudinal elastic oscillations of the tether. Therefore, these two oscillating motions can be investigated by modeling the simplified system as one that consists of one rigid body and one point end-mass, m_1 and m_2, connected by a straight, elastic tether of length l. Such model is used in preliminary tether analyses due to its simplified mathematical representation and computational efficiency. The major assumptions employed in the derivation of the mathematical model are that: 1) the only external force acting on the tether system is the Newtonian gravity force from the target planet. The aerodynamic drag, solar pressure forces, and the gravity from the Sun and other planets are considered negligible, 2) the effect of tether mass is negligible ($m_t = 0$), 3) the tether is fully extended and the reason for the change of tether length is elastic deformation only, 4) the study is carried out for the simpler planar case of motion in the orbital plane, 5) the characteristic size of the spacecraft, $\Delta = D_1 P$ (Figure 1), is much less than length of the tether, $\Delta / l << 1$.

A representation of the model, as well as the generalized coordinates used to describe the motion, are shown in Figure 1. The generalized coordinates are selected as α – the in-plane libration angle of the spacecraft, φ – the in-plane tether libration angle, l – the tether length, θ – the orbit true anomaly of the system's centre of mass, and r – the orbit radius to the system's centre of mass. The equations of motion for the tether system are derived using the Lagrange procedure.

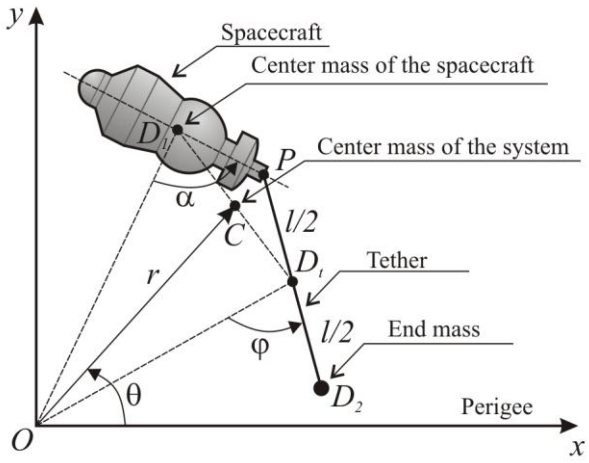

FIGURE 1. Geometry of the tethered system.

Kinetic Energy

In our case kinetic energy may be represented as a sum of three terms

$$T = T_C + T_1 + T_2, \tag{1}$$

where T_C is the kinetic energy of the system's center of mass, T_1 and T_2 is the kinetic energy of the spacecraft and of the end-mass about the system's centre of mass.

Kinetic energy of the system's center of mass orbital motion includes radial and transverse velocity

$$T_C = \frac{1}{2} m\left(\dot{r}^2 + r^2\dot{\theta}^2\right),$$

where $m = m_1 + m_2$ is the total mass of the system. The kinetic energy of the spacecraft about the system's centre of mass can be written as

$$T_1 = \frac{1}{2} m_1 V_{1r}{}^2 + \frac{1}{2} C\omega_1{}^2,$$

where V_{1r} is relative velocity of the spacecraft about the system's centre of mass, ω_1 is the angular velocity of the spacecraft, C is the principal moment of inertia of the spacecraft. The kinetic energy of the end-mass about the system's centre of mass as material point is defined as

$$T_2 = \frac{1}{2} m_2 V_{2r}{}^2,$$

where V_{2r} is relative velocity of the end-mass about the system's centre of mass.
After evaluation and simplification and according to the accepted assumptions kinetic energy of the system [1] with respect to the generalized coordinates may be written as

$$T = \frac{1}{2}m(\dot{r}^2 + r^2\dot{\theta}^2) + \frac{m_*}{2}\dot{l}^2 + \frac{I_*}{2}\left(\dot{\varphi}+\dot{\theta}\right)^2 + \frac{C_1}{2}(\dot{\alpha}+\dot{\theta})^2 + \Delta m_*\left[\dot{l}\sin(\varphi-\alpha) + l(\dot{\varphi}+\dot{\theta})\cos(\varphi-\alpha)\right](\dot{\alpha}+\dot{\theta}), \tag{2}$$

where $m_* = (m_1 m_2)/m$ is defined as the reduced mass of the dumbbell system, $I_* = m_* l^2$ is the moment of inertia of the dumbbell system about the centre of mass of the system, $C_1 = C + m_1\Delta^2$ is the equivalent moment of inertia of the spacecraft.

Potential Energy

The potential energy for the system consists of the gravity potential due to a spherical central planet, of the energy of the dumbbell, the potential energy of the rigid body (spacecraft) in the central force field and the energy of the elastic deformation of the tether

$$W = -\frac{\mu m}{r} + \frac{\mu I_*}{2r^3}\left(1-3\cos^2\varphi\right) + \frac{3\mu}{2r^3}\left(A-B\right)\cos^2\alpha + \frac{c}{2}(l-l_0)^2, \tag{3}$$

where μ is the standard gravitational constant, A and B are the principal moments of inertia of the spacecraft, l_0 is the length of the unstrained tether, $c = E/l_0$, E is modulus of elasticity.

Lagrange procedure and equations of motion

Using expressions (2) and (3), we can write the system's Lagrangian as

$$L = T - W. \tag{4}$$

Now the equations of motion can be obtained via the direct Lagrange procedure:

$$\frac{d}{dt}\left(\frac{dL}{d\dot{q}_j}\right) - \frac{dL}{dq_j} = Q_j, \quad j = \overline{1,5}; \tag{5}$$
$$\left(q_1 = r,\ q_2 = \theta,\ q_3 = l,\ q_4 = \alpha,\ q_5 = \varphi\right)$$

where Q_j is the non-potential force acting along the q_j generalized coordinate. Applying equation (5) to expression (4) we receive five equations of motion of the tethered system

$$C_1\ddot{\alpha}+\left[C_1+\Delta m_* l\cos(\varphi-\alpha)\right]\ddot{\theta}+\Delta m_* l\cos(\varphi-\alpha)\ddot{\varphi}+\Delta m_*\sin(\varphi-\alpha)\ddot{l}$$
$$+2\Delta m_*\dot{l}\left(\dot{\varphi}+\dot{\theta}\right)\cos(\varphi-\alpha)-\Delta m_* l\left(\dot{\varphi}+\dot{\theta}\right)^2\sin(\varphi-\alpha)-\frac{3\mu}{r^3}(A-B)\sin\alpha\cos\alpha=Q_\alpha, \quad (6)$$

$$\Delta m_* l\cos(\varphi-\alpha)\ddot{\alpha}+\left[I_*+\Delta m_* l\cos(\varphi-\alpha)\right]\ddot{\theta}+I_*\ddot{\varphi}+2m_*\dot{l}\left(\dot{\varphi}+\dot{\theta}\right)$$
$$+\Delta m_* l\left(\dot{\alpha}+\dot{\theta}\right)^2\sin(\varphi-\alpha)+\frac{3\mu I_*}{r^3}\sin\varphi\cos\varphi=Q_\varphi, \quad (7)$$

$$\Delta\sin(\varphi-\alpha)\left(\ddot{\alpha}+\ddot{\theta}\right)+\ddot{l}+\frac{c}{m_*}\left(l-l_0\right)+\frac{\mu l}{r^3}\left(1-3\cos^2\varphi\right)-l\left(\dot{\varphi}+\dot{\theta}\right)^2$$
$$-\Delta\left(\dot{\alpha}+\dot{\theta}\right)^2\cos(\varphi-\alpha)=\frac{Q_l}{m_*}, \quad (8)$$

$$\left(mr^2+C_1+I_*\right)\ddot{\theta}+C_1\ddot{\alpha}+I_*\ddot{\varphi}+2mr\dot{r}\dot{\theta}+2m_*\dot{l}\left(\dot{\theta}+\dot{\varphi}\right)=Q_\theta, \quad (9)$$

$$\ddot{r}-r\dot{\theta}^2+\frac{\mu}{r^2}-\frac{3\mu I_*}{2mr^4}\left(1-3\cos^2\varphi\right)-\frac{9\mu}{2mr^4}(A-B)\cos^2\alpha=Q_r, \quad (10)$$

where Q_l is the tether control tension and $\dot{x}=dx/dt$ represents differentiation with respect to time.

Since the orbital time on a hyperbolic orbit is relatively short, it may be assumed that the centre of mass remains in an unperturbed Keplerian hyperbolic orbit. In such a case, the generalized coordinates r and θ are known through

$$r=\frac{p}{k}, \qquad \dot{\theta}=nk^2, \qquad (k=1+e\cos\theta),$$

where $n=\sqrt{\frac{\mu}{p^3}}$, p is the orbit parameter, e is the eccentricity, $x'=dx/d\theta$ represents differentiation with respect to the true anomaly. With these modifications, and taking the independent variable to be the orbit true anomaly, the following three non-dimensional equations of motion are obtained

$$C_1\left(k\alpha''-2e\alpha'\sin\theta\right)+\Delta m_* l\cos(\varphi-\alpha)\left(k\varphi''-2e\varphi'\sin\theta\right)+\Delta m_*\sin(\varphi-\alpha)\left(kl''-2el'\sin\theta\right)+$$
$$+2k\Delta m_* l'\left(1+\varphi'\right)\cos(\varphi-\alpha)-k\Delta m_* l\left(1+\varphi'\right)^2\sin(\varphi-\alpha)-2e\left[C_1+\Delta m_* l\cos(\varphi-\alpha)\right]\sin\theta-$$
$$-3(A-B)\sin\alpha\cos\alpha=\frac{Q_\alpha}{n^2k^3}, \quad (11)$$

$$\Delta m_* l\cos(\varphi-\alpha)\left(k\alpha''-2e\alpha'\sin\theta\right)+I_*\left(k\varphi''-2e\varphi'\sin\theta\right)+2km_* l l'\left(1+\varphi'\right)$$
$$+\Delta km_* l\left(1+\alpha'\right)^2\sin(\varphi-\alpha)-2e\left[I_*+\Delta m_* l\cos(\varphi-\alpha)\right]\sin\theta+3I_*\sin\varphi\cos\varphi=\frac{Q_\varphi}{n^2k^3}, \quad (12)$$

$$\Delta\sin(\varphi-\alpha)\left[k\alpha''-2e\left(1+\alpha'\right)\sin\theta\right]+kl''-2el'\sin\theta+\frac{c}{n^2k^3m_*}\left(l-l_0\right)$$

$$+l\left(1-3\cos^2\varphi\right)-kl\left(1+\varphi'\right)^2-\Delta k\left(1+\alpha'\right)^2\cos(\varphi-\alpha)=\frac{Q_l}{m_* n^2 k^3}. \tag{13}$$

After simplification for the circular orbit ($e=0$), the equations (11) - (13) may be written as

$$C_1\alpha''+\Delta m_* l\cos(\varphi-\alpha)\varphi''+\Delta m_*\sin(\varphi-\alpha)l''+2\Delta m_* l'\left(1+\varphi'\right)\cos(\varphi-\alpha)-$$
$$-\Delta m_* l\left(1+\varphi'\right)^2\sin(\varphi-\alpha)-3\left(A-B\right)\sin\alpha\cos\alpha=\frac{Q_\alpha}{n^2}, \tag{14}$$
$$\Delta m_* l\cos(\varphi-\alpha)\alpha''+I_*\varphi''+2m_* ll'\left(1+\varphi'\right)+\Delta m_* l\left(1+\alpha'\right)^2\sin(\varphi-\alpha)$$
$$+3I_*\sin\varphi\cos\varphi=\frac{Q_\varphi}{n^2}, \tag{15}$$
$$\Delta\sin(\varphi-\alpha)\alpha''+l''+\frac{c}{n^2 m_*}\left(l-l_0\right)+l\left(1-3\cos^2\varphi\right)-l\left(1+\varphi'\right)^2$$
$$-\Delta\left(1+\alpha'\right)^2\cos(\varphi-\alpha)=\frac{Q_l}{m_* n^2}. \tag{16}$$

CHAOTIC OSCILLATIONS OF A SPACECRAFT WITH A VERTICAL TETHER

Let us consider an elastic tethered system, consisting of a spacecraft, an elastic tether and an end-mass in a circular orbit ($e=0$) in the central gravitational field. We will consider the case when the end-mass oscillates on the vertical tether ($\varphi=0$) and the generalized forces $Q_\alpha, Q_l=0$. We will assume that order of magnitude of the following ratios $\delta=\Delta/l$ and $(l-l_0)/l_0$ are equal to $O(\varepsilon)$, where ε is a small parameter. The equations describ the motion of the spacecraft and of the elastic tether (14) and (16) can be written as

$$\alpha''-3\frac{A-B}{C_1}\sin\alpha\cos\alpha=-\delta J\left[\left(1-L''\right)\sin\alpha+2L'\cos\alpha\right], \tag{17}$$
$$L''+\Omega^2 L-\left(3+\Omega^2\right)=\delta\left[\sin\alpha\alpha''+\left(1+\alpha'\right)^2\cos\alpha\right], \tag{18}$$

where $\Omega=\frac{1}{n}\sqrt{\frac{c}{m_*}}$, $L=\frac{l}{l_0}$ is the nondimensional length of the tether, $J=\frac{m_* l_0^2}{C_1}=\frac{m_* l_0^2}{C+m_1\Delta^2}$ is the nondimensional moment of inertia of the tethered system.

If we study the motion of the spacecraft under the influence of the elastic tether by means of equation (17) then we may search for a solution of equation (18) for $\varepsilon=0$

$$L'' + \Omega^2 L - \left(3 + \Omega^2\right) = 0. \tag{19}$$

For the initial conditions:

$$t_0 = 0: \; L = L_1, \; L' = L'_0 \tag{20}$$

solution of equation (19) is given in the form

$$L = L_1 + \frac{L'_0}{\Omega} \sin \Omega\theta, \tag{21}$$

where $L_1 = \dfrac{3 + \Omega^2}{\Omega^2}$. In order for the tether to remain constantly stretched, it is essential that the initial speed of the end-mass (20) is less than the following value

$$L'_0 < \frac{3}{\Omega}.$$

Making use of solution (21) the equation of motion of the spacecraft about of the system's centre of mass (17) could be approximately written by

$$\alpha'' = -a \sin\alpha - c \sin\alpha \cos\alpha - \varepsilon\left(\Omega \sin\alpha \sin\Omega\theta + 2\cos\alpha \cos\Omega\theta\right), \tag{22}$$

where

$$a = \frac{\Delta m_* l_0}{C + m_1 \Delta^2}, \quad c = 3\frac{B - A}{C + m_1 \Delta^2}, \quad \varepsilon = \frac{\Delta m_* l_0 L'_0}{C + m_1 \Delta^2}. \tag{23}$$

If $\varepsilon = 0$ then periodic disturbances are absent, the system (22) remains conservative and describes the motion of the undisturbed biharmonic oscillator as [15]

$$\ddot{\alpha} = -a \sin\alpha - c \sin\alpha \cos\alpha. \tag{24}$$

The coefficient $a > 0$ is always greater than zero, and the sign of c depends on the ratio between the moments of inertia A and B in compliance with (23). Positions of equilibrium of the undisturbed system (24) are defined as roots of the following equation

$$\sin\alpha\left(1 + \gamma \cos\alpha\right) = 0, \tag{25}$$

where $\gamma = ca^{-1}$.

Expression (25) provides solutions for two constant positions of equilibrium:

$\alpha^* = 0, \pi$, and a third position $\alpha^* \in (0, \pi)$ existing only under the condition of

$$|\gamma| > 1. \tag{26}$$

If this condition is not satisfied, then there are only two positions of equilibrium. Point $\alpha^* = 0$ is always a centre, and $\alpha^* = \pi$ - a saddle.

On the other hand, if $\gamma < -1$ then both $\alpha^* = 0, \pi$ and $\alpha^* = \pi$ are saddles, and the intermediate position of equilibrium

$$\alpha^* = \pm \arccos\left(-\gamma^{-1}\right)$$

is a centre (the left branch of the diagram in Figure 2).

If $\gamma > 1$, we see the opposite picture (the right branch of the diagram, Figure 2). The diagram of bifurcations for negative values of α looks like a mirrored transformation relatively to the abscissa axis.

Hyperbolic points (saddles) exist when condition (22) is satisfied. In such cases, the action of external periodic force $\varepsilon\left(\Omega \sin\alpha \sin\Omega\theta + 2\cos\alpha\cos\Omega\theta\right)$ in the disturbed system (22) may lead to chaos and homo/heteroclinic intersections [14]. Chaotic transitions can appear near separatrixes, dividing characteristic areas of motion and connecting hyperbolic points.

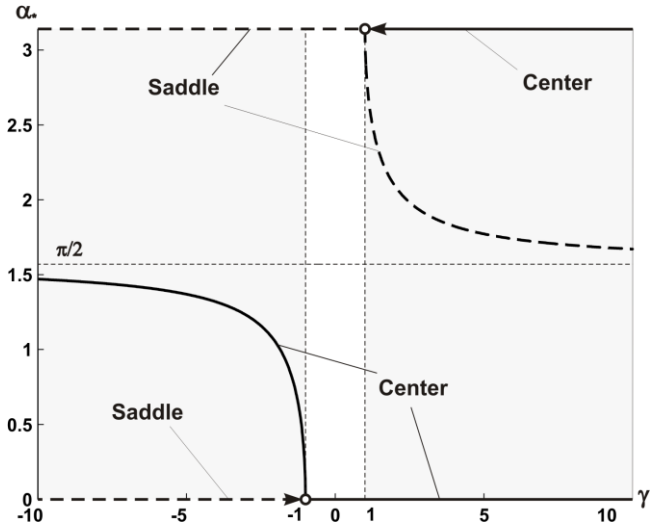

FIGURE 2. Bifurcation diagram of the undisturbed system (24).

Now let us refer to the analysis of the disturbed system (22) by means of the Melnikov method [13]. The Melnikov method is an analytical tool used to define the existence of homo/heteroclinic intersections and as a result of the chaotic behavior. The method provides a necessary condition for the existence of chaos. In order to apply the Melnikov method we need know the analytical solutions of the equation of undisturbed motion at separatrixes.

Solution form varies depending on the values of initial conditions and parameter $\gamma = ca^{-1}$. We consider two cases: $\gamma > 1$ and $\gamma < 1$.

Case 1. If

$$\gamma = ca^{-1} > 1. \tag{27}$$

A case like this results in two unstable – saddle-type points

$$\alpha_S = \pm \arccos\left(-\gamma^{-1}\right), \tag{28}$$

and two stable points – centres

$$\alpha_C = 0, \pm\pi .$$

We can notice, that the centre $\alpha_C = -\pi$ coincides with the center $\alpha_C = \pi$. At the points $\alpha \to -\pi$ and at $\alpha \to \pi$ the speeds α' coincide, therefore we can say, that phase trajectories are closed on a cylindrical phase space. From now on, we can consider the evolution of the cylindrical space in the range of $\alpha \in [-\pi, \pi]$. The phase space can be divided into areas A_0 and A_1, separated by the saddles s_1 and s_{-1} (Figure 3). It is necessary to note that the region A_1 has a discontinuity point $\alpha = \pi, -\pi$. From the expression (28) it follows, that the saddle s_1 belongs to the interval: $\alpha_S \in (\pi/2, \pi)$, and at negative values of $a < 0$ the saddle s_1 belongs to the interval: $\theta_* \in (\pi/2, \pi)$. At $\gamma \to \infty$ we obtain $\alpha_S \to \pi/2$.

The following energy integral corresponds to equation (24):

$$\frac{\alpha'^2}{2} + W(\alpha) = E, \tag{29}$$

where $W(\alpha) = -a\cos\alpha - (c/2)\cos^2\alpha$ is the potential energy and E is the total energy. The shape of the phase portrait depends on the potential energy $W(\alpha)$. The centers α_C correspond to the minimums of the potential energy, and the saddles α_S - to the maximums. If $E > W_S$, where $W_S = W(\alpha_S)$, then the motion is possible in the outer regions (Figure 3). In the opposite case ($E < W_S$) the motion can occur in any of the inner regions, depending on initial conditions. The equality $E = W_S$ corresponds to the motion along separatrixes. In this case, the two saddles s_1 and s_{-1} are connected by four heteroclinic trajectories.

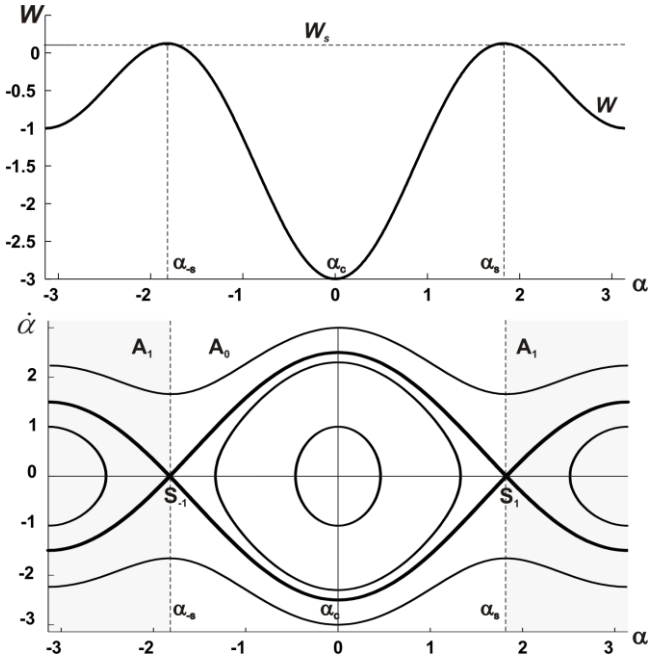

FIGURE 3. Phase space and potential energy plots for the undisturbed system (24) at a=1, c=4.

First of all, we consider the separatrixes, limiting the region A_0. Separating the variables in the energy integral (29), the equation of motion on the separatrixes can be written in the integrated form

$$\theta = \int_{\alpha_0}^{\alpha} \left\{ 2\left[W(\alpha_S) + a\cos\alpha + (c/2)\cos^2\alpha \right] \right\}^{-1/2} d\alpha \ , \tag{30}$$

where $W(\alpha_S) = -a\cos\alpha_S - (c/2)\cos^2\alpha_S = a^2/(2c)$.

Changing the variable

$$x = \tan\alpha/2 \, , \tag{31}$$

simplifies the integral (18) and we obtain the following expression [16]:

$$\theta = 2P^{-1/2}\int_{x_0}^{x}\left(x_1^2 - x^2\right)^{-1} dx = 2P^{-1/2}\ln\left|(x_1+x)/(x_1-x)\right|\Big|_{x_0}^{x} \, ,$$

where $x_1 = \tan(\alpha_S/2)$ and $P = c(c-a)^2 > 0$.

Finally, the solution of equation (24) for the heteroclinic orbits in the region A_0 (Figure 3), can be written as [15]

$$\alpha_{\pm}(\theta) = \pm 2\arctan\left[\tan\left(\alpha_S / 2\right)\tanh\left(\lambda_1\theta / 2\right)\right],$$
$$\sigma_{\pm}(\theta) = (\dot{\alpha})_{\pm} = \pm\lambda_1 \sin\alpha_S \left(\cosh\lambda_1\theta + \cos\alpha_S\right)^{-1}, \tag{32}$$

where $\lambda_1 = \left(c^2 - a^2\right)^{1/2} c^{-1/2}$ is real, if condition (26) is satisfied.

For the area A_1 heteroclinic trajectories have a similar form [15]

$$\alpha_{\pm}(\theta) = \pi \pm 2\arctan\left[\cot\left(\alpha_S / 2\right)\tanh\left(\lambda_1\theta / 2\right)\right],$$
$$\sigma_{\pm}(\theta) = (\dot{\alpha})_{\pm} = \lambda_1 \sin\alpha_S \left(\cosh\lambda_1\theta - \cos\alpha_S\right)^{-1}. \tag{33}$$

Case 2. If

$$\gamma = ca^{-1} < -1, \tag{34}$$

then there are two stable centers

$$\alpha_C = \pm\arccos\left(-\gamma^{-1}\right)$$

and one unstable saddle (Figure 4) $\alpha_S = 0$. In this case the substitution of variables (31) simplifies the integral (30) and results in the following expression

$$\theta = a^{-1/2}\int_{x_0}^{x} x^{-1}\left(x_2^2 - x^2\right)^{-1/2} dx = -\lambda_2^{-2}\ln\left\|\left[x_2 + \left(x_2^2 - x^2\right)^{1/2}\right] / x\right\|_{x_0}^{x}, \tag{35}$$

where $\lambda_2 = \left(-a - c\right)^{1/2}$, $x_2 = \left[-\left(a + c\right) / a\right]^{1/2}$.

Two homoclinic trajectories are symmetrical to the right and to the left of the hyperbolic point $\alpha_S = 0$ (Figure 4). Let us consider only the right orbit. Making a reversed substitution of variables (31) in expression (35) we obtain the following solutions

$$\alpha_{\pm}(\theta) = \pm 2\arctan\left(x_2 / \cosh\lambda_2\theta\right),$$
$$\sigma_{\pm}(\theta) = (\dot{\alpha})_{\pm} = \mp 2\lambda_2 x_2 \sinh\lambda_2\theta / \left[\left(\cosh\lambda_2\theta\right)^2 + x_2^2\right]. \tag{36}$$

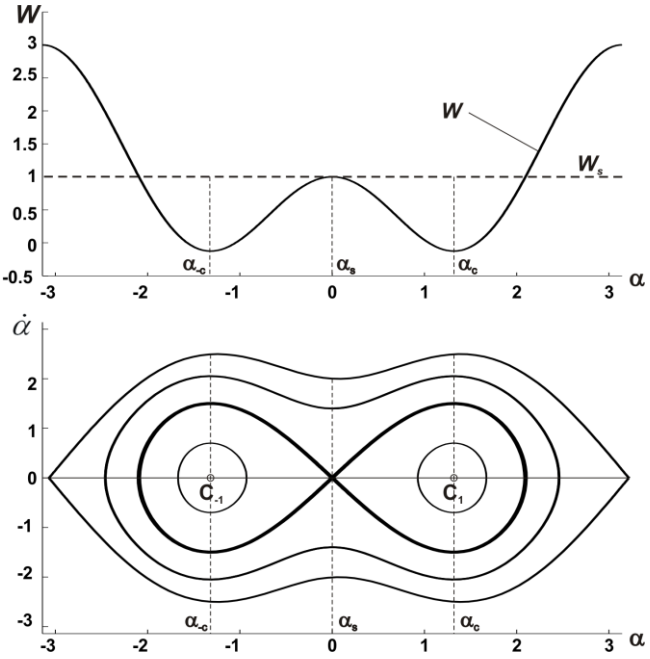

FIGURE 4. Phase space and potential energy plots for the undisturbed system (24) at a=1, c=-4.

The Melnikov function

Stable and unstable manifolds do not necessarily coincide and it is possible for them to cross transversally, leading to an infinite number of new heteroclinic points. Then, a heteroclinic tangle is generated. In such case, as a result of disturbance, the motion of the system (22) near the undisturbed separatrixes becomes chaotic. Inside this chaotic layer small isolated regions of regular motion with periodic orbits can also appear. The existence of heteroclinic intersections may be proved by means of the Melnikov method [13]. We present a more convenient way of using the Melnikov method, applying it to a system of two first order differential equations instead of one disturbed equation of the second order (22)

$$\begin{aligned} &\alpha' = \sigma = f_1 + g_1, \\ &\sigma' = -a\sin\alpha - c\sin\alpha\cos\alpha - \varepsilon\left(\Omega\sin\alpha\sin\Omega\theta + 2\cos\alpha\cos\Omega\theta\right) = f_2 + g_2, \end{aligned} \tag{37}$$

where

$$\begin{aligned} &f_1 = \sigma, \quad f_2 = -a\sin\alpha - c\sin\alpha\cos\alpha, \\ &g_1 = 0, \quad g_2 = -\varepsilon\left(\Omega\sin\alpha\sin\Omega\theta + 2\cos\alpha\cos\Omega\theta\right). \end{aligned} \tag{38}$$

The Melnikov function [13] for system (37) is given as

$$M^{\pm}(\theta_0) = \int_{-\infty}^{\infty} \{ f_1[q_{\pm}^0(\theta)]\ g_2[q_{\pm}^0(\theta), \Omega(\theta+\theta_0)] - f_2[q_{\pm}^0(\theta)]\ g_1[q_{\pm}^0(\theta), \Omega(\theta+\theta_0)]\} d\theta = \int_{-\infty}^{\infty} \{ f_1[q_{\pm}^0(\theta)]\ g_2[q_{\pm}^0(\theta), \Omega(\theta+\theta_0)]\} d\theta, \tag{39}$$

where $q_{\pm}^0(\theta) = [\alpha_{\pm}(\theta), \sigma_{\pm}(\theta)]$ are the solutions at the undisturbed homo/heteroclinic orbits (32), (33) or (36).

The Melnikov function (39) subject to expression (38) can be written as

$$M^{\pm}(\theta_0) = -\varepsilon \int_{-\infty}^{\infty} \sigma_{\pm}\ [\Omega \sin\alpha_{\pm} \sin(\Omega\theta + \Omega\theta_0) + 2\cos\alpha_{\pm} \cos(\Omega\theta + \Omega\theta_0)] d\theta = -\varepsilon \cos\Omega\theta_0 \left(\Omega \int_{-\infty}^{\infty} \sigma_{\pm} \sin\alpha_{\pm} \sin\Omega\theta d\theta + 2\int_{-\infty}^{\infty} \sigma_{\pm} \cos\alpha_{\pm} \cos\Omega\theta d\theta \right). \tag{40}$$

Integrals from of the expression (40)

$$I(\Omega) = -\int_{-\infty}^{\infty} \sigma_{\pm} \sin\alpha_{\pm} \sin\Omega\theta d\theta\,, \tag{41}$$

$$J(\Omega) = \int_{-\infty}^{\infty} \sigma_{\pm} \cos\alpha_{\pm} \cos\Omega\theta d\theta \tag{42}$$

define the amplitude of changes in the thickness of chaotic layer. We can calculate its absolute size for three orbits:

two heteroclinic orbits (32) and (33) - case 1,

one homoclinic orbit (36) - case 2.

Integrals (41) and (42) have identical structure, therefore further we will consider only the integral (41). Substituting the solutions (32), (33) and (36) into the integral (41), we obtain three integrals in the form of functions of a dimensionless frequency of the external disturbance

$$I_0(\Omega_1) = \sin^2\alpha_S \int_{-\infty}^{\infty} \frac{\sinh\tau_1}{(\cosh\tau_1 + \cos\alpha_S)^2} \sin(\Omega_1\tau_1) d\tau_1, \tag{42}$$

$$I_1(\Omega_1) = \sin^2\alpha_S \int_{-\infty}^{\infty} \frac{\sinh\tau_1}{(\cosh\tau_1 - \cos\alpha_S)^2} \sin\Omega_1\tau_1 d\tau_1, \tag{43}$$

$$I_2(\Omega_2) = 2x_2^2 \int_{-\infty}^{\infty} \frac{\sinh(2\tau_2)}{\left(\cosh^2\tau_2 + x_2^2\right)^2} \sin\Omega_2\tau_2 d\tau_2, \tag{44}$$

where $\tau_1 = \lambda_1\theta$, $\tau_2 = \lambda_2\theta$ is the dimensionless time, $\Omega_1 = \Omega\lambda_1^{-1}$ and $\Omega_2 = \Omega\lambda_2^{-1}$ are the dimensionless frequencies.

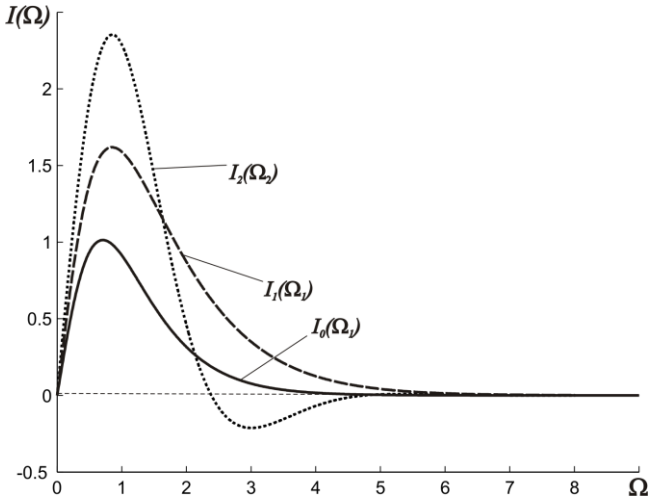

FIGURE 5. Evolution of the maximum thickness of chaotic layers (42), (43) and (44) as the functions of dimensionless frequencies $\Omega_1 = \Omega\lambda_1^{-1}$ and $\Omega_2 = \Omega\lambda_2^{-1}$

We can notice, that according to (23), the natural frequencies $\lambda_1 = \left(c^2 - a^2\right)^{1/2} c^{-1/2}$ and $\lambda_2 = \left(-a - c\right)^{1/2}$ depend on the parameters of the tethered system and on inertia moments of the spacecraft. We have analyzed the evolution of the maximum thickness of the chaotic layers for the homo/heteroclinic orbits (32), (33) and (36) as the functions of the dimensionless frequencies Ω_1 and Ω_2. Calculations, based on the numerical integration of (42)-(44) show, that at $\Omega_1, \Omega_2 > 6$ the thickness of chaotic layer tends to zero (Figure 5), therefore the regular structure of a phase space of the disturbed system (22) is observed and trajectories have no homo/heteroclinic intersections (Figure 5). It means, that at $\Omega_1, \Omega_2 > 6$ the disturbed force $\varepsilon\left(\Omega \sin\alpha \sin\Omega\theta + 2\cos\alpha \cos\Omega\theta\right)$ has no influence on the behavior of the disturbed system (22).

CONCLUSION

This work attempts to describe transient cases of motion of a spacecraft with an elastic tether deployed on a local vertical using the methods of chaotic mechanics, particularly, the Melnikov method. We have established the borders of homo/heteroclinic chaos using the Melnikov method, which allows us to choose tethered systems parameters that will ensure regular behavior of the spacecraft with elastic tether in motion around the centre of mass.

ACKNOWLEDGMENTS

This research was supported by the Russian Foundation for Basic Research (09-01-00384).

REFERENCES

1. V.V. Beletsky and E.M. Levin, *Dynamics of space tether systems*, Univelt, Inc., San Diego, 1993, p. 499.
2. P. Williams, C. Blanksby and P. Trivailo, Tethered planetary capture: controlled maneuvers. *Acta Astronautica*, 2003, v. 53, pp. 681–708.
3. P. Williams, Spacecraft Rendezvous on Small Relative Inclination Orbits Using Tethers, *Journal of Spacecraft and Rockets*, V. 42, N. 6, 2005 pp. 1047-1060.
4. F. Zimmermann, U. Schottle and E. Messerschmid, Optimization of the tether-assisted return mission of a guided re-entry capsule. *Aerospace Science and Technology*, 2005, v. 9. № 8, pp.713–721.
5. F. Dignath and W. Schiehlen, Control of the vibrations of a tethered satellite system, *Journal of Applied Mathematics and Mechanics*, v. 64, is. 5, 2000, pp. 715–722.
6. A.K. Misra, Dynamics and control of tethered satellite systems. *Acta Astronautica*, 2008, v. 63, pp. 1169–1177.
7. M. Kruijff and E. Van der Heide, Qualification and in-flight demonstration of a European tether deployment system on YES2. *Acta Astronautica*, 2009, v. 64, pp. 882–905.
8. P. Williams, A. Hyslopb, M. Stelzerb and M. Kruijff, YES2 optimal trajectories in presence of eccentricity and aerodynamic drag, *Acta Astronautica*, v. 64, 2009, pp. 745–769.
9. P. Williams, Dynamics and Control of Spinning Tethers for Rendezvous in Elliptic Orbits, *Journal of Vibration and Control*, v. 12, 2006, pp. 737–771.
10. V. Aslanov, The oscillations of a body with an orbital tethered system, *Journal of Applied Mathematics and Mechanics*, v. 71, is. 6, 2007, pp. 926-932.
11. V. Aslanov, The Oscillations of a Spacecraft under the Action of the Tether Tension Moment and the Gravitational Moment, *AIP (American Institute of Physics),* Conf. Proc. September 1. 2008. v. 1048, pp. 56-59.
12. D.Arnold, The behavior of long tethers in space, *The Journal of the Astronautical Sciences*, v. 35, is. 1, 1987, pp.3-18.
13. V.K. Melnikov, On the stability of the center for time periodic perturbations, *Trans. Moscow Math. Soc.*, v. 12, 1963, pp. 1–56.
14. J. Guckenheimer and P. Holmes, *Nonlinear oscillations, dynamical and bifurcations of vector fields*, Springer-Verlag, 1986.
15. V. Aslanov, Chaotic behavior of the biharmonic dynamics system, *International Journal of Mathematics and Mathematical Sciences (IJMMS)*, paper 319179, 2009. http:// www.hindawi.com/journals/ijmms/.
16. I.S. Gradshteyn and I.M. Ryzhik, *Table of integrals, Series and Products*, Academic Press, San Diego, 1980.